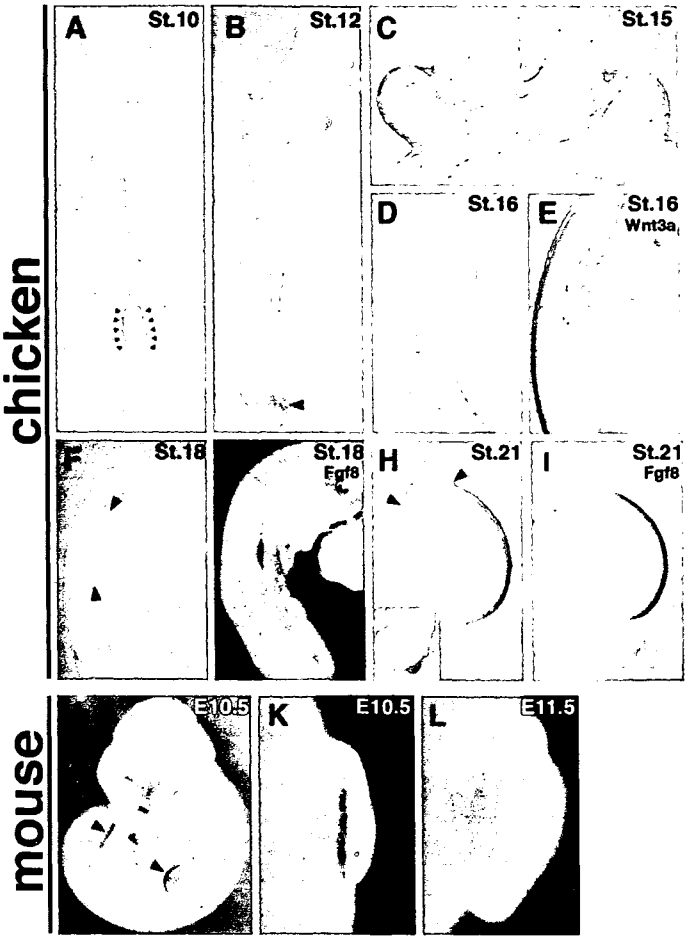

Fig. 2.

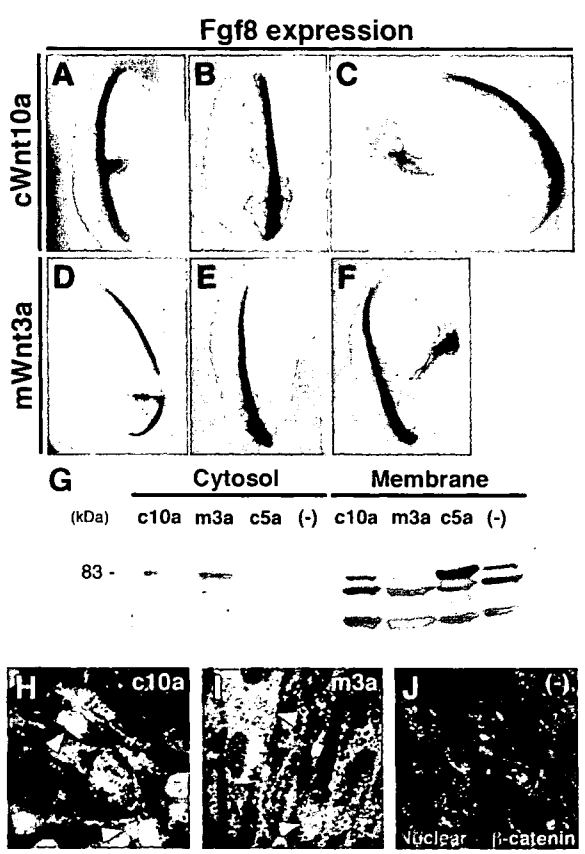

Fig. 3.

Fig. 2. *Wnt10a* is localized in the apical ectodermal ridge (AER) in chick and mouse embryos. A–I: Chicken embryo. J–L: Mouse embryo. **A,B:** Expression of *Wnt10a* at stage (St.) 10 (A) and 12 (B), respectively. Dorsal view of the whole embryo. The expression is observed broadly in the surface ectoderm and strongly in the surface ectoderm along the neural folds of the closing neural tube (A, arrowheads) and around the tail bud (B, arrowhead). **C:** Expression of *Wnt10a* at stage 15. A cross-section at a prospective forelimb level, showing dorsal on the top. The expression is observed in the surface ectoderm overlying the lateral plate mesoderm. **D,E:** Expression of *Wnt10a* and *Wnt3a*, respectively, at stage 16. E: *Wnt3a* is also expressed in the dorsal neural tube. Lateral view of the prospective forelimb region, showing dorsal on the left. **F,G:** Expression of *Wnt10a* and *Fgf8*, respectively, at stage 18. *Wnt10a* expression becomes strong at the region between arrowheads. Lateral view of the forelimb and the trunk regions. **H,I:** Expression of *Wnt10a* and *Fgf8*, respectively, at stage 21. Lateral view of the forelimb. H, window: A cross-section through the AER. H: *Wnt10a* expression is observed in the AER and weakly in the nonridge ectoderm (arrowheads) but is not detected in the limb mesenchyme (window). J,K: Expression of *Wnt10a* at 10.5 days post coitum. *Wnt10a* expression is localized in the forelimb and hindlimb AER (arrowheads). **J:** Lateral view of the whole embryo. Ventral view of the forelimb bud. **K:** Dorsal on the right. **L:** Expression of *Wnt10a* at 11.5 days post coitum. Ventral view of the forelimb bud. Dorsal on the right.

Fig. 3. Wnt10a can induce ectopic *Fgf8* expression and activate the Wnt/β-catenin signaling. **A–F:** Misexpression of chick Wnt10a (cWnt10a, A–C) or mouse Wnt3a (mWnt3a, D–F) using replication-competent retroviral vector in the developing chick limb bud. Expression of *Fgf8* in the injected limb bud. Dorsal is on the left. In cWnt10a misexpression, ectopic *Fgf8* expression is observed in the ectoderm lateral to the apical ectodermal ridge (AER,A,B) or distant to the AER (C, 8/13), as well as in mWnt3a misexpression (D–F). **G:** Western blot analysis of β-catenin in the cytoplasmic and membrane fractions of chicken embryonic fibroblasts (CEFs), expressing excess Wnt proteins. Cytoplasmic β-catenin levels are elevated in CEFs overexpressing chicken *Wnt10a* and mouse *Wnt3a*, compared with in those overexpressing chicken *Wnt5a* and control CEFs. Left, position of a molecular weight marker protein. c10a, chicken *Wnt10a*; m3a, mouse *Wnt3a*; c5a, chicken *Wnt5a*; (−), control CEFs alone. H–J: Detection of nuclear β-catenin on CEFs expressing Wnts. **H,I:** In Wnt10a (H) or mouse Wnt3a (I) misexpression, β-catenin (green) is observed in the nucleus (red) in addition to accumulated cytoplasmic β-catenin. The arrowheads indicate the areas of β-catenin and nucleus colocalization (yellow). **J:** In contrast, β-catenin is undetectable in the nucleus in control CEFs.

Wnt10a Induces Ectopic *Fgf8* Expression in the Chick Limb Bud

During AER formation, *Wnt10a* signals were first detected intensely in the surface ectoderm of the presumptive limb field, and subsequently in the AER, suggesting that *Wnt10a* is involved in AER formation during chick limb development. To test this possibility, we carried out *Wnt10a* misexpression studies in the chick limb bud using the replication-competent retroviral vector (RCAS). RCAS-Wnt10a viruses were injected into the presumptive limb field of stage 11–13 embryos. Exogenous *Wnt10a* was misexpressed in the developing limb bud and led to ectopic *Fgf8* expression in the limb ectoderm adjacent or distant to the AER (Fig. 3A–C, 8/13). Similar results were obtained by misexpressing mouse *Wnt3a* in the chick limb bud (Fig. 3D–F).

Wnt10a Activates the Wnt/β-Catenin Signaling Pathway

The β-catenin signaling is known to be critical for AER formation during vertebrate limb development. To test whether Wnt10a can activate the β-catenin signaling pathway, we examined accumulation of cytoplasmic β-catenin in chicken embryonic fibroblasts (CEFs). Overexpression of *Wnt10a* triggered an increase in cytoplasmic β-catenin levels, compared with the control (Fig. 3G). The increasing levels of β-catenin induced by Wnt10a were approximately equal to those induced by mouse Wnt3a (Fig. 3G). Wnt5a, which does not activate β-catenin signaling, did not accumulate β-catenin in CEFs, as previously reported (Shimizu et al., 1997; Kawakami et al., 2001).

Cytoplasmic β-catenin is translocated into the nucleus and in association with LEF/TCF transcriptional factors regulates transcription of the target genes. We examined whether Wnt10a promoted translocation of β-catenin into the nucleus. RCAS constructs were transfected into CEFs, and then anti–β-catenin antibody and propidium iodide were added to detect β-catenin protein and the nucleus, respectively. Distributions of β-catenin protein (green) and the nucleus (red) into the cells were analyzed using a confocal laser-scanning microscope. In CEFs expressing *Wnt10a* or mouse *Wnt3a*, β-catenin protein was detected within the nucleus (yellow, Fig. 3H,I, arrowheads). In contrast, no β-catenin protein was detected within the nucleus in control CEFs (Fig. 3J). These results indicated that Wnt10a activated the β-catenin signaling pathway in AER formation.

DISCUSSION

In this study, we isolated the Wnt10a gene in chicken embryo and identified *Wnt10a* expression pattern in both chicken and mouse embryos (Figs. 1, 2). We also found that Wnt10a promotes cytoplasmic accumulation and nuclear distribution of β-catenin (Fig. 3G–J), indicating that it triggers the β-catenin signaling pathway. We showed that *Wnt10a* misexpression leads to ectopic *Fgf8* expression (Fig. 3A–C). We also discussed the roles of Wnt10a in AER formation in the chick and mouse.

Wnt10a and Wnt3a in Chicken Embryo

Wnts and Fgfs play a key role in the genetic cascade that controls limb development. First, *Wnt2b/8c* is expressed in the lateral plate mesoderm of the presumptive limb fields and induces *Fgf10* expression in the lateral mesoderm (Kawakami et al., 2001). Fgf10 induces *Wnt3a* expression in the overlying ectoderm (Kawakami et al., 2001). Then, Wnt3a promotes *Fgf8* expression in the surface ectoderm, which maintains *Fgf10* expression in the underlying mesenchyme (Ohuchi et al., 1997a; Kengaku et al., 1998).

We found that *Wnt10a* expression started with the same timing as *Wnt3a*. Although we tested whether *Wnt10a* expression is induced by the implantation of cells expressing Fgf10 in the flank region, *Wnt10a* was not detected after 24 hr (data not shown). *Wnt3a* induction, on the other hand, was observed after 24 hr (data not shown). Therefore, *Wnt10a* expression may be regulated directly by a more-upstream factor such as Wnt2b/8c or Tbx5/4, which is involved in induction of the forelimb/hindlimb (Kawakami et al., 2001; Takeuchi et al., 2003).

On the basis of an analysis of its overexpression and expression patterns, Wnt3a is considered a candidate of AER inducers, because mouse *Wnt3a* was able to induce ectopic *Fgf8* expression when misexpressed in the chick limb bud (Kengaku et al., 1998). *Wnt10a* as well as *Wnt3a* leads to ectopic *Fgf8* expression. During AER formation, *Wnt10a* expression overlaps that of *Wnt3a*. *Wnt10a* expression becomes strong in the presumptive limb ectoderm at stage 16 before *Fgf8* expression. *Wnt3a* expression is first detected in the region at stage 16 (Kengaku et al., 1997). The expression of *Wnt10a* and *Wnt3a* is maintained until stage 27. However, there is a difference in the duration of *Wnt10a* and *Wnt3a* expression in the AER. Although *Wnt10a* expression continues until stage 32, *Wnt3a* expression becomes undetectable at stage 29. In addition, *Wnt10a* is not expressed in the dorsal neural tube, proximal otic vesicle, and feather buds, whereas *Wnt3a* is detected in these regions (Hollyday et al., 1995; Chang et al., 2004). These observations suggest that Wnt10a function is redundant with that of Wnt3a in induction of *Fgf8* expression.

Wnt10a and *Wnt3* in Mouse Embryo

Mouse *Wnt3*, an AER inducer, is expressed ubiquitously in the limb ectoderm (Parr et al., 1993; Barrow et al., 2003). Because the AER is localized at the dorsal–ventral border, this means that other Wnt members and/or more factors, such as bone morphogenetic protein signaling molecules, are also involved in AER formation (Barrow et al., 2003; Soshnikova et al., 2003). *Wnt10a* expression is localized in developing AER in both mice and chickens. In addition, overexpression of mouse Wnt10a led to ectopic *Fgf8* expression in chicken embryos (data not shown). These data suggest that Wnt10a is also involved in AER formation. To elucidate the role of Wnt10a in AER formation, analysis of the targeted disruption of the Wnt10a gene in mice is needed.

EXPERIMENTAL PROCEDURES

Chicken Embryos

Fertilized chicken eggs were incubated at 38°C. The embryos were staged according to Hamburger and Hamilton (1951). Chicken embryo fibroblasts were cultured in Dulbecco's modified Eagle medium (D-MEM) containing 2% fetal bovine serum (FBS) and 1% chicken serum.

Cloning of Chicken *Wnt10a*

To isolate chicken *Wnt10a* cDNA, we first screened genomic libraries using mouse *Wnt10a* as a probe. To isolate full-length cDNA, we performed 5'-RACE (Invitrogen). The sequence was determined and deposited to the GenBank/DDBJ with the accession number AB177400.

Plasmid Constructions

To carry out misexpression in CEFs and in the developing limb bud, the full coding regions of chicken *Wnt10a* and mouse *Wnt3a* were subcloned into RCAS L14 or L44 (Kawakami et al., 1996). The RCAS construct for chicken *Wnt5a* has been reported previously (Kawakami et al., 1999).

In Situ Hybridization

A plasmid containing the entire coding region of chicken *Wnt10a* was digested with *Nsi*I followed by blunting and was transcribed with T3 RNA polymerase to prepare the antisense probe. Antisense RNA probes for chicken *Fgf8* (Ohuchi et al., 1997b) and chicken *Wnt3a* (Kawakami et al., 2000) had been synthesized previously. Embryos were fixed in 4% paraformaldehyde (PFA) in PBS at 4°C overnight and dehydrated in ethanol. Whole-mount in situ hybridization was performed, as described previously (Kawakami et al., 1996). Stained embryos were embedded in 0.5% gelatin/30% albumin and sectioned with a Vibratome at 30–50 μm.

Western Analysis

Cytoplasmic β-catenin accumulation assay was carried out using a method previously described (Shimizu et al., 1997; Kawakami et al., 2001). CEFs were transfected with the RCAS constructs. Samples containing 50 μg of total protein were subjected to electrophoresis through sodium dodecyl sulfate-polyacrylamide (7.5%) gels. The primary antibody against β-catenin (BD Transduction Lab.) was used at a dilution of 1:2,000. The protein was detected using the ECL Plus System (Amersham Pharmacia Biotech) with a 1/10 dilution of the reagent mixture.

Detection of Nuclear β-Catenin

CEFs were transfected with the RCAS constructs and cultured on cover glasses until the cultures became confluent. After fixation in 4% PFA in PBS at room temperature for 15 min, cells were treated with 50% methanol in PBS at 4°C for 5 min. After incubation with 20 μg/ml RNase A in PBS at 37°C for 30 min, cells were treated with 1% bovine serum albumin in PBS at room temperature for 60 min. The primary antibody against β-catenin (BD Transduction Lab.) was used at a dilution of 1:2,000 at 4°C overnight. The secondary antibody (fluorescein isothiocyanate conjugate) against mouse-IgG was used at a dilution of 1:1,000 at room temperature for 60 min. The nuclei were stained with 50 μg/ml propidium iodide at room temperature for 2 min. The cells were observed using a confocal laser-scanning microscope.

Misexpression in Chick Limb Buds

Preparation of the retroviruses bearing the *Wnt* genes was performed according to the method of Fekete and Cepko (1993). The RCAS construct was transfected into DF-1 cells (ATCC; #CRL-12203) using Lipofectamine 2000 (Invitrogen). Cells were grown in the culture medium (5% FBS and 1% chicken serum in D-MEM). After confluence in a 15-cm culture dish, the medium was replaced with 20 ml of fresh medium (2% FBS and 0.5% chicken serum in D-MEM). On the next day, the medium was harvested and replaced. The medium was pooled after four replacements. To concentrate the virus particles in the culture medium, the medium was centrifuged at 4°C for 10 min at 3,000 × *g*. The supernatant was filtered through a membrane with a pore size of 0.45 μm (Whatmann; 6896-2504). After the medium was centrifuged again at 4°C for 3 hr at 70,000 × *g*, the major part of the medium was discarded by decantation and the virus particles in the bottom pellet were resuspended in a small volume of the remaining medium (approximately 200 μl). The final titer of the virus was usually 180- to 240-fold concentration.

Virus infection was carried out using Line M, retrovirus-free, fertilized chicken eggs (Nisseiken). The retrovirus was injected into the presumptive limb fields on the right side of stage 10–13 embryos. After 1.5–2 days of reincubation, the embryos were fixed in 4% PFA in PBS and the gene expression pattern was determined using in situ hybridization.

ACKNOWLEDGMENTS

We thank Ms. C. Komaguchi-Wada and A. Shiga-Oda for technical assistance. We also thank D.H. Waterbury for critical reading of the manuscript.

REFERENCES

Barrow JR, Thomas KR, Boussadia-Zahui O, Moore R, Kemler R, Capecchi MR, McMahon AP. 2003. Ectodermal Wnt3/beta-catenin signaling is required for the establishment and maintenance of the apical ectodermal ridge. Genes Dev 17: 394–409.

Chang CH, Jiang TX, Lin CM, Burrus LW, Chuong CM, Widelitz R. 2004. Distinct Wnt members regulate the hierarchical morphogenesis of skin regions (spinal tract) and individual feathers. Mech Dev 121:157–171.

Fekete DM, Cepko CL. 1993. Replication-competent retroviral vectors encoding alkaline phosphatase reveal spatial restriction of viral gene expression/transduction in the chick embryo. Mol Cell Biol 13:2604–2613.

Galceran J, Farinas I, Depew MJ, Clevers H, Grosschedl R. 1999. Wnt3a$^{(-/-)}$-like phenotype and limb deficiency in Lef1$^{(-/-)}$Tcf1$^{(-/-)}$ mice. Genes Dev 13:709–717.

Hamburger V, Hamilton HL, 1951. A series of normal stages in the development of the chick embyo. J Morphol 88:49–92.

Hollyday M, McMahon JA, McMahon AP. 1995. Wnt expression patterns in chick embryo nervous system. Mech Dev 52:9–25.

Kawakami Y, Ishikawa T, Shimabara M, Tanda N, Enomoto-Iwamoto M, Iwamoto M, Kuwana T, Ueki A, Noji S, Nohno T. 1996. BMP signaling during bone pat-

tern determination in the developing limb. Development 122:3557–3566.

Kawakami Y, Wada N, Nishimatsu S, Ishikawa T, Noji S, Nohno T. 1999. Involvement of Wnt-5a in chondrogenic pattern formation in the chick limb bud. Dev Growth Differ 41:29–40.

Kawakami Y, Wada N, Nishimatsu S, Nohno T. 2000. Involvement of frizzled-10 in Wnt-7a signaling during chick limb development. Dev Growth Differ 42: 561–569.

Kawakami Y, Capdevila J, Buscher D, Itoh T, Rodriguez-Esteban C, Izpisua-Belmonte JC. 2001. WNT signals control FGF-dependent limb initiation and AER induction in the chick embryo. Cell 104: 891–900.

Kengaku M, Twombly V, Tabin C. 1997. Expression of Wnt and Frizzled genes during chick limb bud development. Cold Spring Harb Symp Quant Biol 62:421–429.

Kengaku M, Capdevila J, Rodriguez-Esteban C, De La Pena J, Johnson RL, Belmonte JC, Tabin CJ. 1998. Distinct WNT pathways regulating AER formation and dorsoventral polarity in the chick limb bud. Science 280:1274–1277.

Ohuchi H, Nakagawa T, Yamamoto A, Araga A, Ohata T, Ishimaru Y, Yoshioka H, Kuwana T, Nohno T, Yamasaki M, Itoh N, Noji S. 1997a. The mesenchymal factor, FGF10, initiates and maintains the outgrowth of the chick limb bud through interaction with FGF8, an apical ectodermal factor. Development 124:2235–2244.

Ohuchi H, Shibusawa M, Nakagawa T, Ohata T, Yoshioka H, Hirai Y, Nohno T, Noji S, Kondo N. 1997b. A chick wingless mutation causes abnormality in maintenance of Fgf8 expression in the wing apical ridge, resulting in loss of the dorsoventral boundary. Mech Dev 62:3–13.

Parr BA, Shea MJ, Vassileva G, McMahon AP. 1993. Mouse *Wnt* genes exhibit discrete domains of expression in the early embryonic CNS and limb buds. Development 119:247–261.

Shimizu H, Julius MA, Giarre M, Zheng Z, Brown AM, Kitajewski J. 1997. Transformation by Wnt family proteins correlates with regulation of beta-catenin. Cell Growth Differ 8:1349–1358.

Soshnikova N, Zechner D, Huelsken J, Mishina Y, Behringer RR, Taketo MM, Crenshaw EB III, Birchmeier W. 2003. Genetic interaction between Wnt/beta-catenin and BMP receptor signaling during formation of the AER and the dorsal-ventral axis in the limb. Genes Dev 17: 1963–1968.

Takeuchi JK, Koshiba-Takeuchi K, Suzuki T, Kamimura M, Ogura K, Ogura T. 2003. Tbx5 and Tbx4 trigger limb initiation through activation of the Wnt/Fgf signaling cascade. Development 130:2729–2739.

顎顔面形態形成に関与するWntファミリーの発現パターン

山本　康弘，高田　温行，森口　隆彦，和田　直之*，本間　隆義*，
濃野　勉*

ニワトリ胚の顎顔面形成過程において，分泌性タンパク質であるWntファミリーの発現パターンをin situ hybridizationで調べた．脊椎動物で19個あるWntメンバーのうち，Wnt-3a，Wnt-5a，Wnt-10a，Wnt-11が顎顔面の形態形成で発現していた．Wnt-5aは発生が進むとともに各顔面隆起の遠位側先端に強く発現していた．また，Wnt-11はそれぞれの顔面隆起間の近接部間充織に強く発現していた．一方，Wnt-3aとWnt-10aは上皮でのみ発現していた．これらの時間的，空間的に特異的な発現パターンから，これらのWntファミリーが顎顔面の骨格や筋分化に至る過程で分化誘導シグナルとして重要な働きをしていると考えられる．
（平成17年9月8日受理）

Expression Pattern of the Wnt Family During Orofacial Development in the Chicken Embryo

Yasuhiro YAMAMOTO, Haruyuki TAKATA, Takahiko MORIGUCHI,
Naoyuki WADA*, Takayoshi HONMA* and Tsutomu NOHNO*

The expression pattern of the secretion glycoprotein Wnt family during orofacial development in the chicken embryo was observed by in situ hybridization. From among the 19 members of the Wnt family, Wnt-3a, Wnt-5a, Wnt-10a, and Wnt-11 were expressed in the processes during orofacial development in the embryo. Wnt-5a was strongly expressed in the mesenchymal cells in the distal region of the facial processes. Expression of Wnt-11was restricted to the region where the processes fuse with each other at later stage. Wnt-3a and Wnt-10a were expressed broadly in the surface ectoderm of the processes. These spatio-temporal expression patterns suggest that these Wnt proteins play important roles in skeletal and muscular differentiation.(Accepted on September 8, 2005) *Kawasaki Igakkaishi 31(1)：97－105, 2005*

Key Words ① **Wnt-5a** ② **Wnt-11** ③ **Chicken embryo**
④ **Orofacial development**

川崎医科大学　形成外科
〒701-0192 倉敷市松島577

*分子生物学
e-mail address：yyasu8310@go9.enjoy.ne.jp

Department of Plastic and Reconstructive Surgery, Kawasaki Medical School：577 Matsushima, Kurashiki, Okayama 701-0192 Japan
Department of Molecular Biology

はじめに

胚発生における顎顔面の形態形成は第1鰓弓(first branchial arch)背方部の上顎隆起(maxillary prominence), 第1鰓弓腹方部の下顎隆起 (mandibular prominence), および前脳胞腹方部の前頭鼻隆起 (frontonasal prominence) から始まる. 顔面の中心部を構成する口窩は, その側縁周囲を構築する一対の上顎隆起, 口窩の下縁を構築する一対の下顎隆起, および口窩の上縁を構築する無対の前頭鼻隆起からなる (**Fig. 1**). 顎顔面を構成する骨格は顔面隆起内を満たす神経堤細胞に由来する間充織が分化して形成される. 上顎隆起の間充織は膜性骨化により顎前骨 (premaxilla), 上顎骨 (maxilla), 頬骨 (zygomatic bone), および側頭骨 (temporal bone) の一部を形成する. 一方, 下顎隆起では間充織の膜性骨化により下顎骨 (mandible) が形成される. 前頭鼻隆起の両側に鼻板 (nasal placode) とよばれる体表外胚葉の局所的肥厚があり, 発生が進むと鼻板は陥入して卵円形の鼻窩 (nasal pit) となる. この際に鼻窩の周囲に馬蹄形の隆起が生じ, この内側部が内側鼻隆起 (medial nasal prominence), 外側部が外側鼻隆起 (lateral nasal prominence) である. 発生が進むとともに, 上顎隆起は外側鼻隆起と癒合し頬と上顎骨を形成する. また, 上顎隆起が前方に増大し内側鼻隆起とも癒合し, 上唇と顎前骨を形成する. 一対の下顎隆起は正中線上で癒合し, 下唇と下顎を形成する[1),2)]. これら顔面隆起の形成や増殖の異常, また隆起間の癒合不全などにより, 口唇裂口蓋裂などの顔面奇形が生ずると考えられている[3)].

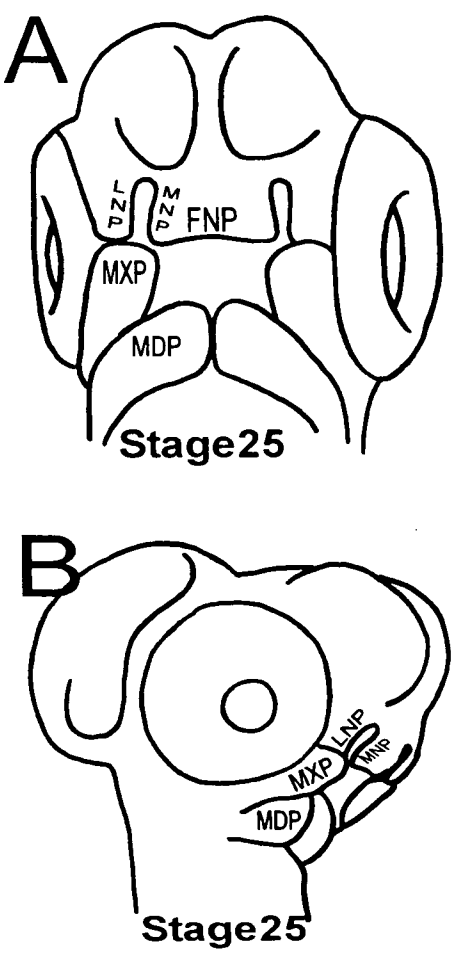

Fig. 1. Facial prominences of the chicken embryo.
(**A**) Frontal view. (**B**) Side view. Abbreviations : MXP, maxillary prominence ; MDP, mandibular prominence ; FNP, frontonasal prominence ; LNP, lateral nasal prominence ; MNP, medial nasal prominence.

一方, 顎顔面形成過程には, 多数の分子やそれらの相互作用が関与することが報告されている. 特に, 細胞間の情報伝達を担う分泌性タンパク質は, 位置特異的な顔面隆起の発達や間充織細胞の増殖分化, 器官形成に至るまでのさまざまな発生段階と部位で機能することが理解されている. 現在のところ, TGF-β や SHH, BMP, FGF など, 多くの器官において重要な機能を果たす分子が顎顔面形成にも関与することが報告されている[4)~6)]. その一方で多様な役割が報告されている分泌性糖タンパク質の1つである Wnt ファミリーについては, 初期胚の軸性決定, 胚葉分化, 後脳の形成, 神経管や体節の分化, 四肢や腎臓の形成などにおける役割についてよく調べられている[7)~17)]が, 顎顔面の形成での役割については不明であり, その発現パターンも体系的に調べられていない. そこで私達は, 口唇裂口蓋裂の分子的メカニズムを調べる一環として[6),18),19)], 顎顔面形態形成における Wnt の役割を解明するために, ニワトリ胚でその発現パターンを調べた.

実験材料と方法

1．ニワトリ受精卵

発生stageはHamburger and Hamilton（1951）に従った[20]．発現パターンを調べるためにwhole-mount in situ hybridizationを行った．また，約5日胚（stage 26）の上顎隆起および下顎隆起を含む切片を作成し，切片でのin situ hybridizationを行った．In situ hybridizationのためprobeにはWnt-3a, Wnt-4, Wnt-5a, Wnt-7a, Wnt-8c, Wnt-10a, Wnt-11のcDNAを用いた．In situ hybridizationには自動ISH装置（ALOKA AIH-101）を使用した．

2．受精卵の培養

レトロウイルス非感染のニワトリ受精卵は日生研㈱より購入し，38℃の孵卵器（SANYO INCUBATOR MIR-153）で4日（stage 23前後），5日（stage 25前後），6日（stage 28前後）まで孵卵した．

3．胚の固定と脱水

胚を卵から採りだし，phosphate-buffered saline（PBS）を満たしたシャーレの上で羊膜を剥ぎ，胸腹部臓器を除去した後，4% paraformaldehyde／PBS溶液に置換し4℃で一晩固定した．4% paraformaldehyde／PBS溶液を0.1% Tween 20を含むPBS溶液（PBT）に置換し，10分間振盪した．その後，25% ethanol／PBTで5分，50% ethanol／PBTで5分，75% ethanol／PBTで5分，100% ethanolで5分それぞれ振盪した．最後に再度100% ethanolで10分間振盪した後，−20℃で保存した．（100% ethanol以外は全てRNase-freeの水を使用した．）

4．Whole-Mount in situ hybridization

試料の入っている100% ethanolを75% ethanol／PBTに置換し，5分間振盪し再水和を行った．その後，50% ethanol／PBTで5分間，25% ethanol／PBTで5分間，PBTで5分間それぞれ振盪した後，再度PBTに置換し5分間振盪した．Proteinase K／PBT溶液（2μg/ml）に置換し，37℃で15分間振盪した．その後，glycine（2 mg/ml）／PBT溶液に置換後，室温で5分間，PBTで2回5分間振盪した．2% gluteraldehyde + 4% paraformaldehyde／PBT溶液に置換し，20分間振盪した．その後，PBTに置換し5分間振盪した（2回繰り返す）．PBTに置換し，68℃で50分間振盪した．その後，十分に冷却したPBTに置換し，氷上で5分間振盪した．6% H_2O_2／methanol溶液に置換し，氷上で1時間振盪した．その後，PBSで5分間，PBTで5分間振盪後，68℃のpre-hybridization mix（組成：50% formamide, 5× SSC pH 7.0, 50μg/ml tRNA, 1% SDS, 50μg/ml heparin）に置換し，1時間振盪した．

Digoxigenin（DIG）- labeled RNA probe（0.5μg）+希釈用pre-hybridization mix溶液に置換し，68℃で一晩hybridizationを行った．Probeは，滅菌蒸留水（5μl），10× transcription buffer（1μl），10× DIG-RNA labeling mixture（1μl），RNase inhibitor（1μl），Linearized template DNA（1μl），RNA polymerase（1μl）を混合し，37℃で2時間反応して合成した．DIG標識RNAは必要に応じて限定的アルカリ分解で断片化して用いた．

Hybridization wash solution 1（組成：5× SSC, 50% formamide, 1% SDS）に置換し，軽く振盪した．再度，新たなhybridization wash solution 1に置換し，68℃で30分間振盪し洗浄を行った．その後，hybridization wash solution 2（組成：2× SSC, 50% formamide, 0.1% Tween20）で5分間，さらに同じ液を用いて68℃で30分間，さらにTBST（組成：100 mM Tris-HCl pH 7.5, 150 mM NaCl, 0.1% Tween 20）で室温5分間を3回繰り返し，ブロッキング溶液（組成：1× TBST, 1.5% Blocking reagent）で60〜90分間，それぞれ振盪した．最後にブロッキング溶液を除き，抗体を加え4℃で一晩振盪し，抗体反応を行った．

TBSTに置換し5分間振盪を4回行った．次に，新たにTBSTに置換して，30分間振盪を8回，NTMT（組成：0.1M NaCl，0.1M Tris-HCl pH 9.5，50 mM $MgCl_2$，0.1% Tween20）に換えて3回，10分間振盪による洗浄を行った．その後，NTMTを発色液（NBT：4-Nitro blue tetrazolium chloride＋BCIP：5-Bromo-4-chloro-3-indolyl-phosphate／NTMT）に換え，発色反応を開始した．発色開始から10分後から発色状況を確認し，発色が完了したところでPBTに置換し，5分間振盪を3回行い，発色反応を停止した．次に50% ethanol／PBTに置換し，5分間振盪後100% ethanolに換え1.5～3時間振盪した．その後，50% ethanol／PBTで5分間，PBTで5分間振盪した後，アルミホイルに包み遮光して4℃で保存した．

5．切片作製

取り出した胚を4% paraformaldehyde／PBS溶液で固定し，脱水，再水和後にパラフィン包埋した．上顎隆起と下顎隆起が含まれる様に額面断で，薄切の厚さは7 μmで切片を作製した．

In situ hybridizationは，4．Whole-Mount in situ hybridizationの手法に準じて行った．変更点としては，pre-hybridization mixにはWhole-Mountで使用したpre-hybridization mixに終濃度10% dextran sulfateを加えたものを使用し，発色液はWhole-Mountの場合の1／10の濃度を用いた．発色停止後に0.1% Nuclear fast red／5%硫酸アルミニウム水溶液で核を染色した．

結　　果

ニワトリ胚の約4日胚(stage 23)，約5日胚(stage 25)，約6日胚（stage 28）を用いて，Wntファミリーのうち Wnt-3a, Wnt-4, Wnt-5a, Wnt-7a, Wnt-8c, Wnt-10a, Wnt-11を調べた．その結果，Wnt-4，Wnt-7a，Wnt-8cについては顔面隆起での発現はほとんどみられなかった．以下，顕著な発現シグナルがみられたWntについて記載する．

1．Wnt-5a

Stage 23では上顎隆起全体に強く発現している．また下顎隆起全体にも発現しているが，遠位で強く近位では弱く発現している．口窩には発現していない．外側鼻隆起および内側鼻隆起にも強く発現しているが，鼻窩には発現していない（**Fig. 2A, B**）．

Stage 25ではstage 23と同様にすべての顔面隆起で発現している．Stage 23に比べ，それらの発現は，隆起の遠位側で強くなっている（**Fig. 2C, D**）．Stage 26胚の上顎隆起および下顎隆起を含む切片より，Wnt-5aの顔面隆起における発現は，間充織のみで上皮（外胚葉）にはみられないことが分かる（**Fig. 2F**）．

さらに発生が進みstage 28では，突出してきた前頭鼻隆起の先端で強く発現している．一方，上顎隆起と下顎隆起での発現は，より先端辺縁部に弱くに局在している（**Fig. 2E**）．

2．Wnt-11

Stage 23では，上顎隆起と下顎隆起の近接部および上顎隆起と外側鼻隆起の近接部で強く発現している．また，眼胞周囲にも強く発現している（**Fig. 3A, B**）．

Stage 25ではstage 23と同様に，上顎隆起と下顎隆起の近接部および上顎隆起と外側鼻隆起の近接部で，より局在化して発現している．また，上顎隆起と内側鼻隆起の近接部にも発現している（**Fig. 3C, D**）．Stage 26胚の上顎隆起および下顎隆起を含む切片より，Wnt-11は，上顎隆起と下顎隆起の近接部の間充織に強く発現している．一方，上皮（外胚葉）での発現は，みられない（**Fig. 3F**）．

さらに発生が進行しstage 28になると，顔面隆起での発現は，消失している（**Fig. E**）．

3．Wnt-3aおよびWnt-10a

両者とも，顎顔面形態形成過程を通して上皮（外胚葉）で発現がみられるが，各々の顔面隆

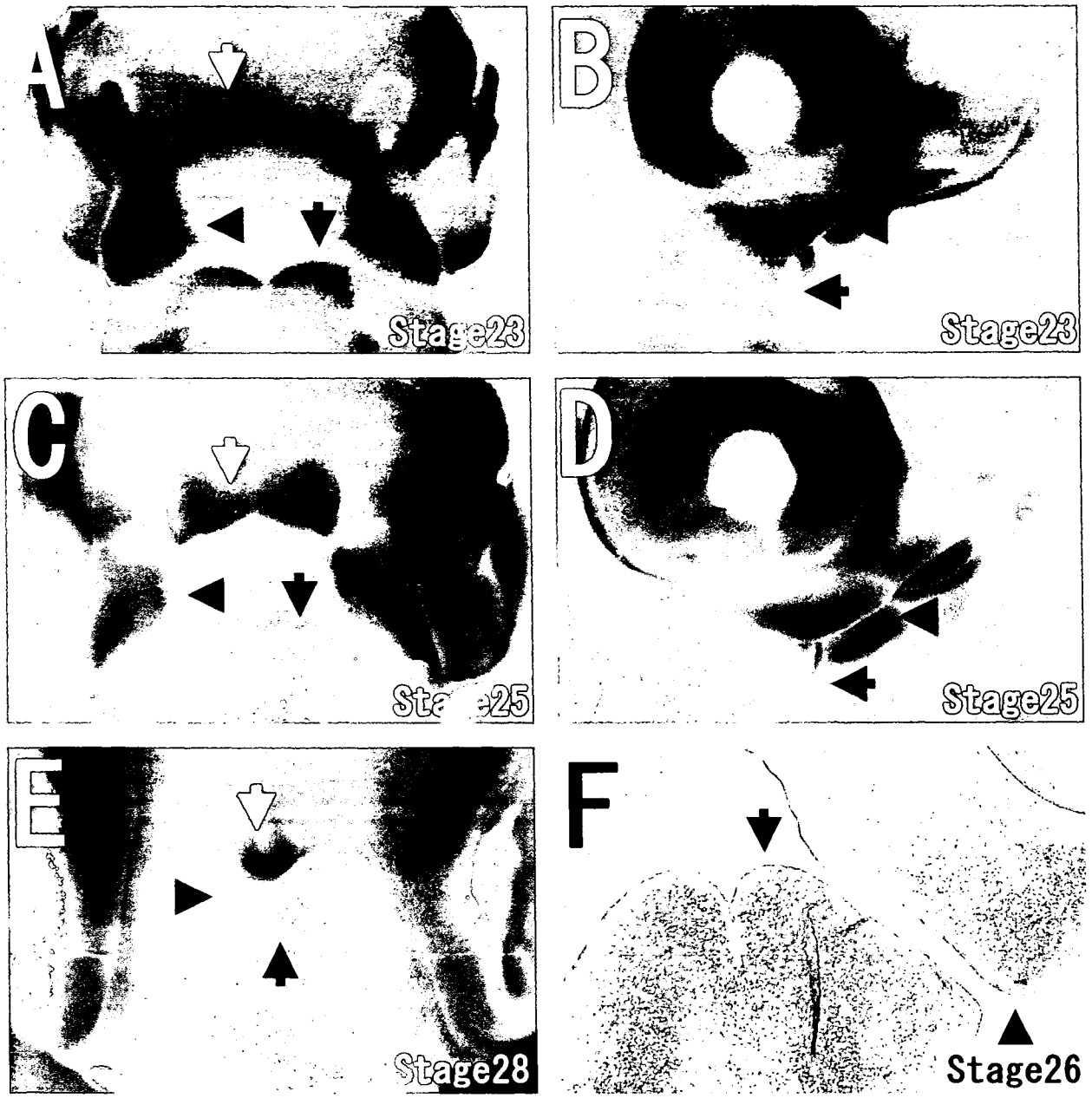

Fig. 2. Expression of the Wnt-5a gene in the facial prominence of the chicken embryo.
(**A, B**) Frontal view (**A**) and side view (**B**) of a day 4 (stage 23) embryo. (**C, D**) Frontal view (**C**) and side view (**D**) of a day 5 (stage 25) embryo. (**E**) Frontal view of a day 6 (stage 28) embryo. (**F**) Frontal section of a day 5 (stage 26) embryo after Nuclear fast red staining. (×20). (**A–D**) Wnt-5a is expressed in the frontonasal prominences (white arrows), the maxillary prominences (black arrows) and the mandibular prominences (black arrowheads) of embryos at stages 23 to 25. (**E**) Wnt-5a expression decreases in the distal region of the maxillary and mandibular prominences at stage 28 embryo, while strong expression continues at the tip of the frontonasal prominence. (**F**) Wnt-5a is expressed in mesenchymal cells of the maxillary and mandibular prominences, but not in the surface ectoderm.

起において強い局所的な発現はない．両者を比較すると，Wnt-3aに比べWnt10aの方がやや強い発現シグナルがみられた（**Fig. 4A–D**）．

考　　察

Wntファミリーは分子量約4万の糖タンパク質であり，ショウジョウバエのセグメントポラリティ遺伝子群の1つwinglessと，マウス

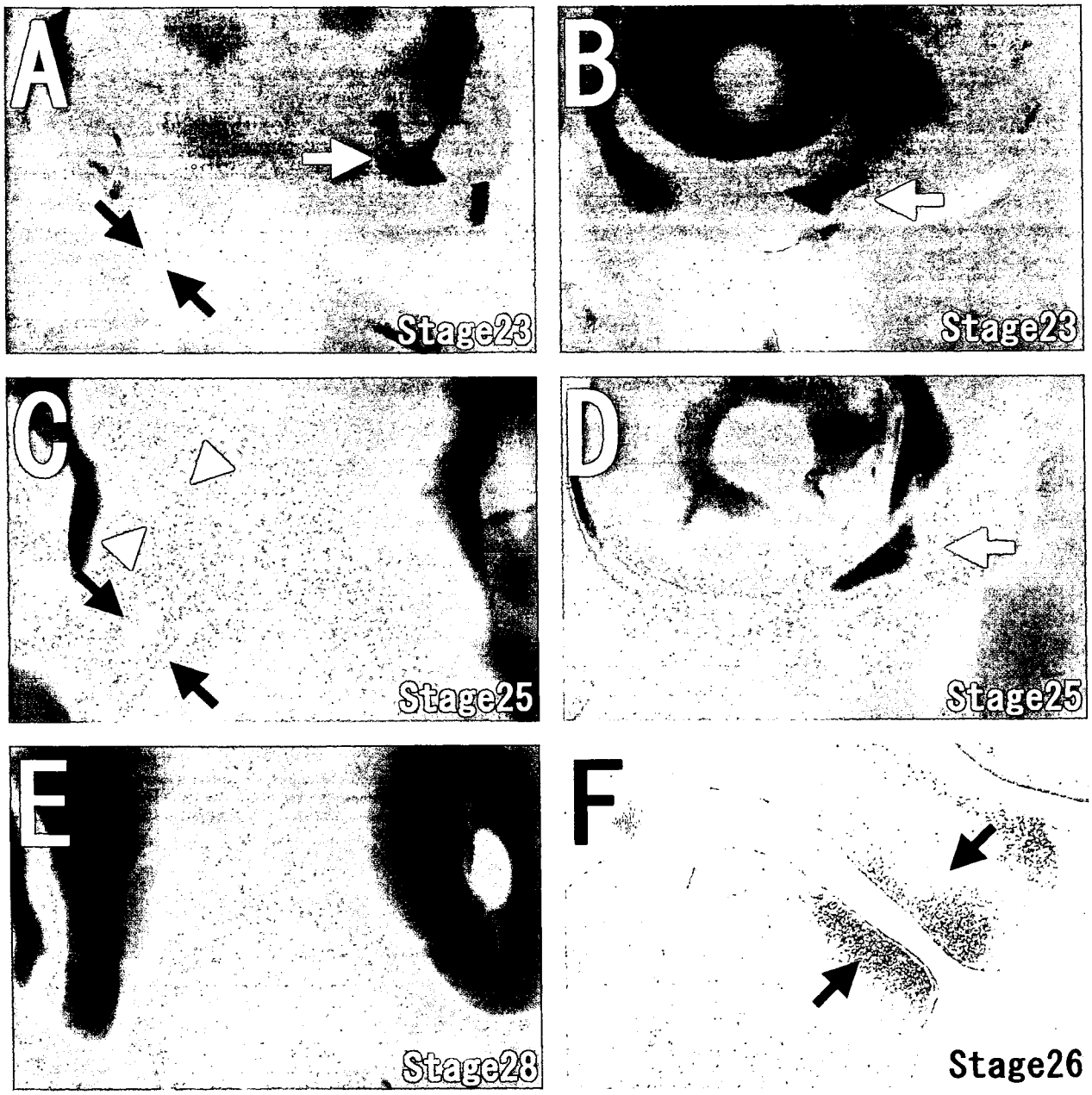

Fig. 3. Expression of the Wnt-11 gene in the facial prominence of the chicken embryo.
(**A**, **B**) Frontal view (**A**) and side view (**B**) of a day 4 (stage 23) embryo. (**C**, **D**) Frontal view (**C**) and side view (**D**) of a day 5 (stage 25) embryo. (**E**) Frontal view of a day 6 (stage 28) embryo. (**F**) Frontal section of a day 5 (stage 26) embryo after Nuclear fast red staining. (×20). (**A-D**) Wnt-11 is expressed at stages 23 to 25 in the restricted region where the maxillary prominence and the mandibular prominence become contacted (black arrows), in the region where the maxillary prominence and the lateral nasal prominence become contacted (white arrows), and in the region where the maxillary prominence and the medial nasal prominence become contacted (white arrowheads). Wnt-11 is expressed in the mesenchymal region surrounding the optic vesicle. (**E**) Expression becomes faint during orofacial development. (**F**) Expression of Wnt-11 is observed in the mesenchymal region where the maxillary and mandibular prominences become contacted (black arrows).

乳癌で同定された癌遺伝子 int-1との構造が類似していたことに基づいて，総称して Wnt と呼ばれるようになった．現在，脊椎動物では19種のメンバーが知られており，さまざまな局面で時間的，位置的に特異的な発現を示し，形態形成の誘導因子，細胞の極性決定因子，増殖分化の調節因子として機能している[7),8)]．

Wnt-5a は四肢が成長していく際，肢芽先端の間充織の増殖と伸長に関与すると考えられている[21),22)]．ここで観察された結果からも Wnt

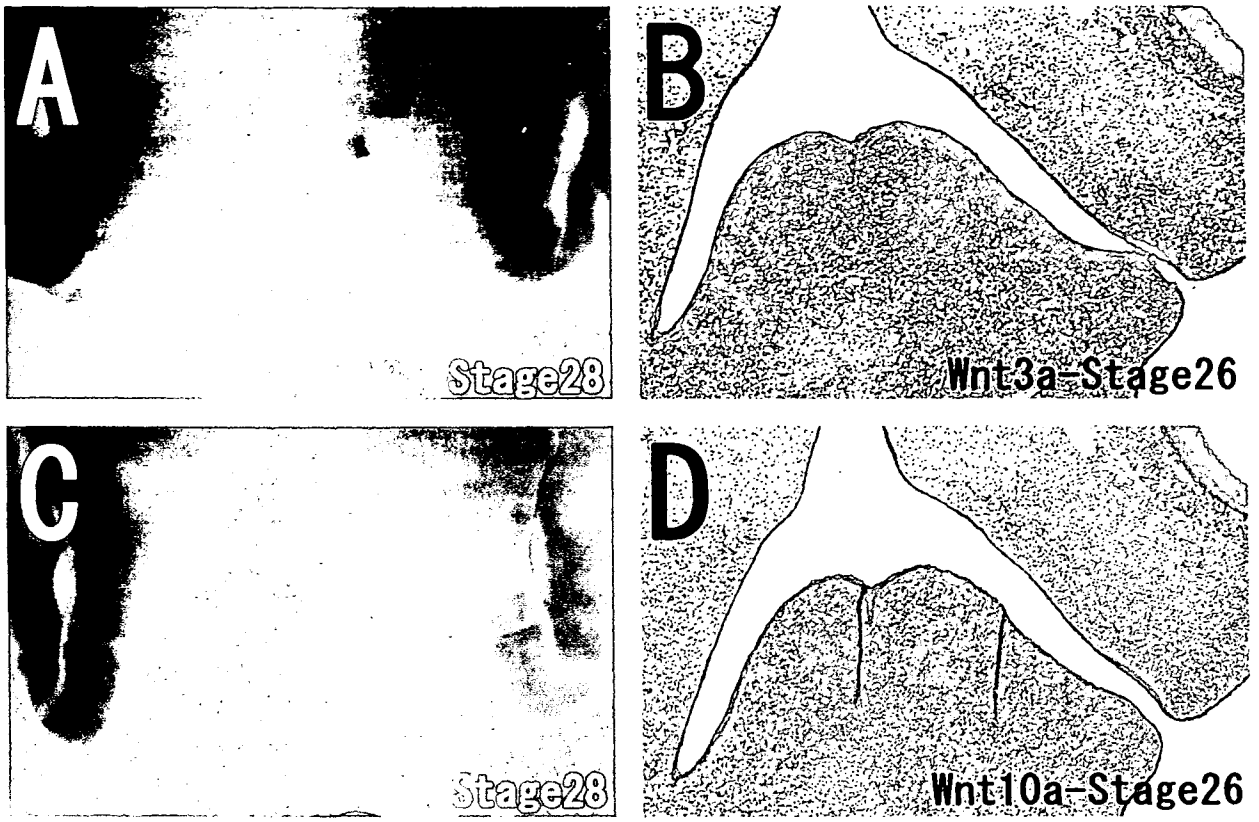

Fig. 4. Expression of Wnt-3a and Wnt-10a in the facial prominence of the chicken embryo.
(**A**, **B**) Wnt-3a. (**C**, **D**) Wnt-10a. (**A**) Frontal view of a day 6 (stage 28) embryo. (**B**) Frontal section of a day 5 (stage 26) embryo after Nuclear fast red staining. (×20). (**C**) Frontal view of a day 6 (stage 28) embryo. (**D**) Frontal section of a day 5 (stage 26) embryo after Nuclear fast red staining. (×20). (**A**, **C**) Wnt-3a and Wnt-10a are weakly expressed in the ectoderm of the maxillary and frontonasal prominence. (**B**, **D**) Expression of Wnt-3a and Wnt-10a are detected in the ectoderm of the mandibular prominence.

-5aはstageが進むとともに，顔面隆起の遠位側で強い発現があり，同部位の間充織における増殖と伸長に関与すると考えられる．しかし，Wnt-5aは非βカテニン経路のCa^{2+}経路を主として作動することが知られており[12]，細胞分化には関与するが直接の細胞増殖シグナルとは考えられていない．四肢の形成において，Wnt-5aは軟骨分化，筋肉分化に関与していることが調べられており[9),10),21]，またWnt-5aのノックアウトマウスでは四肢の先端部への伸展が阻害されることが知られている[22]．従って，Wnt-5aの顎顔面の形成過程での発現パターンから，ここでも四肢の場合と同様に，顎の軟骨分化や筋肉分化に関与している可能性が考えられる．

Wnt-11は初期胚において非βカテニン経路の1つであるJNK経路を介して平面内細胞極性の決定や細胞分化に関与していることが知られている[11),12]．また，上顎隆起と内側鼻隆起の癒合には，TGF-βやSHH，FGF，BMPのシグナルが関与し，これらの因子はJNK経路とのシグナルクロストークが知られている[11]．ここで得られた結果ではWnt-11が上顎隆起と下顎隆起の近接部および上顎隆起と外側鼻隆起の近接部で強く発現していた．従って，癒合に関与する上記シグナルに加え，Wnt-11も上顎隆起下顎隆起間と上顎隆起外側鼻隆起間など，それぞれの顔面隆起の癒合に関与し，単なる隆起の伸展から顔面の形態形成に至る過程に関与する因子の一つであると考えられる．

おわりに

口唇裂口蓋裂の分子的メカニズムを調べる一環として，形態形成に関わる分泌性タンパク質

の中でWntファミリーに注目し，ニワトリ胚の顎顔面形成過程でその発現パターンをin situ hybridizationで調べた．その結果，TGF-β，SHH，FGF，BMPに加えWnt-5aやWnt-11も関与していることが判明した．顎顔面形態形成におけるWntの役割については，過剰発現による機能亢進や欠損型による機能低下の影響を調べるなど，更なる解析が必要である．口唇裂口蓋裂をはじめ，顔面裂の分子メカニズムを解明するために，Wnt-11やWnt-5aは有効な分子マーカーとなるだけでなく，作用型ペプチドや抑制型ペプチドを鰓弓で過剰発現することなどで影響を調べ，機能を明らかにすることが今後の課題となる．

謝　辞

実験にご協力いただいた寺田久美子さん，内田恵美さん，磯田恵子さんに感謝いたします．

本研究の一部はプロジェクト研究費（14-101，14-206，15-103A，15-216B，16-101M，16-209T），文部科学省の科学研究費（13680813，14034260，16027251），両備檉園記念財団助成金によって行われた．

参考文献

1) Sadler TW：ラングマン人体発生学．第8版．安田峯生，野沢十蔵，訳．東京，メディカル・サイエンス・インターナショナル，319－353，2001
2) Larsen WJ：ラーセン最新人体発生学．第2版．相川英三，山下和雄，三木明徳，大谷浩，訳．新潟，西村書店，315－338，1999
3) 森口隆彦，中川皓文，森　寿子：口唇裂口蓋裂の総合治療－成長に応じた諸問題の解決－．東京，克誠堂出版，18-27，1995
4) Francis-West P, Ladher R, Barlow A, Graveson A：Signalling interactions during facial development. Mech Dev 75：3－28，1998
5) Lee SH, Bedard O, Buchtova M, Fu K, Richman JM：A new origin for the maxillary jaw. Dev Biol 276：207－224，2004
6) Stanier P, Moore GE：Genetics of cleft lip and palate：syndromic genes contribute to the incidence of non-syndromic cleft. Hum Mol Genet 13：R73－R81，2004
7) 濃野　勉：Wntファミリーと形態形成．現代医療 32：1912－1921，2000
8) 濃野　勉：骨形成にかかわるWntシグナリング．実験医学 20：2469－2476，2002
9) Church V, Nohno T, Linker C, Marcelle C, Francis-West P：Wnt regulation of chondrocyte differentiation. J Cell Sci 115：4809－4818，2002
10) Anakwe K, Robson L, Hadley J, Buxton P, Church V, Allen S, Hartmann C, Harfe B, Nohno T, Brown AM, Evans DJ, Francis-West P：Wnt signalling regulates myogenic differentiation in the developing avian wing. Development 130：3503－3514，2003
11) 笹岡俊輔，宇田川潔，濃野　勉：Wntシグナリング．生体の科学 55：464－465，2004
12) 中村　勉，秋山　徹：Wntシグナルネットワークの多彩な生理機能．生化学 77：5－19，2005
13) Narita T, Sasaoka S, Udagawa K, Ohyama T, Wada, N, Nishimatsu S, Takada S, Nohno T：Wnt10a is involved in AER formation during chick limb development. Dev Dyn 233：282－287，2005
14) Kengaku M, Capdevila J, Rodriguez-Esteban C, De La Pena J, Johnson RL, Izpisua-Belmonte J-C, Tabin CJ：Distinct WNT pathways regulating AER formation and dorsoventral polarity in the chick limb bud. Science 280：1274－1277，1998
15) Tanda N, Ohuchi H, Yoshioka H, Noji S, Nohno T：A chicken Wnt gene, Wnt-11, is involved in dermal development. Biochem Biophys Res Commun 211：123－129，1995

16) Logan CY, Nusse R：The Wnt signaling pathway in development and disease. Annu Rev Cell Dev Biol. 20：781－810, 2004

17) Nelson WJ, Nusse R：Convergence of Wnt, β－catenin, and Cadherin pathways. Science 305：1483－1487, 2004

18) MacDonald ME, Abbott UK, Richman JM：Upper beak truncation in chicken embryos with the cleft primary palate mutation is due to an epithelial defect in the frontonasal mass. Dev Dyn 230：335－349, 2004

19) McGonnell IM, Clarke JD, Tickle C：Fate map of the developing chick face：analysis of expansion of facial primordia and establishment of the primary palate. Dev Dyn 212：102－118, 1998

20) Hamburger V, Hamilton H：A series of normal stages in the development of the chick embryo. J Morph 88：49－92, 1951

21) Kawakami Y, Wada N, Nishimatsu S, Ishikawa T, Noji S, Nohno T：Involvement of Wnt-5a in chondrogenic pattern formation in the chick limb bud. Dev Growth Differ 41：29－40, 1999

22) Yamaguchi TP, Bradley A, McMahon AP, Jones S：A Wnt5a pathway underlies outgrowth of multiple structures in the vertebrate embryo. Development 126：1211－1223, 1999

FEBS Letters 580 (2006) 4463–4468

Bone marrow transplantation improves outcome in a mouse model of congenital muscular dystrophy

Hiroki Hagiwara[a], Yutaka Ohsawa[a], Shoji Asakura[b], Tatsufumi Murakami[a], Takanori Teshima[c], Yoshihide Sunada[a,*]

[a] *Division of Neurology, Department of Internal Medicine, Kawasaki Medical School, 577 Matsushima, Kurashiki-City, Okayama 701-0192, Japan*
[b] *Biopathological Science, Okayama University Graduate School of Medicine and Dentistry, 2-5-1 Shikata-cho, Okayama-City, Okayama 700-8558, Japan*
[c] *Center for Cellular and Molecular Medicine, Kyushu University Hospital, 3-1-1, Maidashi, Higashi-ku, Fukuoka-City, Fukuoka 812-8582, Japan*

Received 23 April 2006; revised 10 June 2006; accepted 3 July 2006

Available online 14 July 2006

Edited by Jesus Avila

Abstract **We examined whether pathogenesis in dystrophin-deficient (*mdx*) mice and laminin-α2-deficient (*dy*) mice is ameliorated by bone marrow transplantation (BMT). Green fluorescent protein (GFP) mice were used as donors. In *mdx* mice, BMT failed to produce any significant differences in muscle pathology, although some GFP-positive fibers with restored dystrophin expression were observed. In contrast, in the *dy* mice, BMT led to a significant increase in lifespan and an increase in growth rate, muscle strength, and respiratory function. We conclude that BMT improved outcome in *dy* mice but not *mdx* mice.**

Keywords: Bone marrow transplantation; Muscular dystrophy; *mdx* mouse; *dy* mouse; Laminin α2; Basal lamina

1. Introduction

The muscular dystrophies are groups of inherited myogenic disorders characterized by progressive muscle wasting and weakness of variable distribution and severity. Two major types of severe muscular dystrophy, Duchenne muscular dystrophy (DMD) and congenital muscular dystrophy, have been identified [1]. DMD is caused by mutations of the dystrophin gene [2]. Most cases of congenital muscular dystrophy are caused by mutations in the laminin-α2 chain (merosin) gene. This disease has been termed merosin-deficient congenital muscular dystrophy (MCMD) or MDC1A [3]. Pathogenesis of dystrophin-deficient or laminin-α2-deficient muscular dystrophy can be studied in mouse models [4]. Loss of dystrophin protein is observed in the *mdx* mouse, the mouse model of DMD [5]. The *dystrophia muscularis* (*dy*) mouse has spontaneous mutation in the *Lama2* gene encoding laminin-α2 and is used as a model of MDC1A [6,7]. Although some potential treatments including pharmacologic methods, gene therapy, and cell therapy have been tried, there are no effective therapeutic approaches for muscular dystrophy at present [8].

Bone marrow transplantation (BMT) is an established clinical procedure used to treat various human diseases. Adult bone marrow (BM) cells contain mesenchymal stem cell progenitors, which can give rise to osteocytes, chondrocytes, adipocytes, and myocytes [9,10]. BM is also a promising source of myogenic stem cells [11]. Recently, several investigators have reported that transplanted BM cells participate in the muscle regeneration process in irradiated recipient mice [12–15] or DMD patient [16]. However, analyses of these studies are often limited to histopathologic assessments.

In the present study, we examined the therapeutic effect of whole BMT on muscular dystrophy model mice by evaluating clinical phenotypes such as body weight, lifespan, muscle strength, and respiratory function as well as histopathology. We also compared the therapeutic effect of whole BMT on two distinct models of muscular dystrophy, *mdx* and *dy* mice. Our results showed that BMT improved outcome in *dy* mice but failed to affect pathology of *mdx* mice. Thus a therapeutic approach of transplanting BM cells could be considerable benefit in MDC1A.

2. Materials and methods

2.1. Mice

The C57BL/6 (wild-type) mice were purchased from Clea Japan (Tokyo, Japan). The *mdx* mice (of C57BL/10 background) were provided by Central Institute for Experimental Animals (Kanagawa, Japan). The laminin-α2-deficient *Lama2−/−* mice (*dy*) mice and the EGFP transgenic (GFP-Tg) mice with a C57BL/6 background [17] were purchased from Jackson Laboratory (Bar Harbor, Maine, USA). All experiments involving animals were performed under the guidelines of the Institutional Animal Care and Research Advisory Committee, Kawasaki Medical School.

2.2. Bone marrow reconstitution

BM chimeras were established by following the method of Fukada et al. [15] with modifications. Briefly, adult (8-week-old) wild-type, *mdx* or *dy* mice received 9 Gy TBI (X-ray), split into two doses separated by 3 h to minimize gastrointestinal toxicity. BMT was performed according to a standard protocol described previously [18,19]. Recipient mice were injected with 5×10^6 T cell-depleted BM cells. T cell depletion of donor BM cells was performed using anti-CD90-MicroBeads and an AutoMACS system (Miltenyi Biotec, Auburn, CA, USA) according to the manufacturer's instructions. No unfavorable results such as GVHD were observed in recipient mice received BM cells from GFP mice.

*Corresponding author. Fax: +818 6462 1199.
E-mail address: ysunada@med.kawasaki-m.ac.jp (Y. Sunada).

Abbreviations: BMT, bone marrow transplantation; DMD, Duchenne muscular dystrophy; MDC1A, congenital muscular dystrophy type 1A; SpO_2, arterial hemoglobin saturation

0014-5793/$32.00
doi:10.1016/j.febslet.2006.07.015

2.3. Histology and immunohistochemistry

Cryosections of diaphragm muscle were prepared as described previously [20]. For immunohistochemical analysis, sections were immunostained with a rabbit polyclonal antibody against GFP (MBL, Nagoya, Japan) or a monoclonal antibody against C-terminus of dystrophin (NCL-DYS2; Novocastra, Newcastle, United Kingdom), laminin-α2 (merosin) (clone 4H8-2; Sigma–Aldrich, St. Louis, MO, USA) followed by fluorescein isothiocyanate-conjugated secondary antibodies according to the MOM procedure (Vector Laboratories, Burlingame, CA, USA). The slides were mounted with VECTASHIELD plus DAPI (Vector Laboratories). The fluorescence images were recorded photographically using a microscope (Nikon, Tokyo, Japan) and analyzed with Lumina Vision software (Mitani Corporation, Fukui, Japan).

2.4. Grip strength test and pulse oximetry

Peak grip strength (g) was measured using an MK-380S automated grip strength meter (Muromachi Kikai, Tokyo, Japan) as described previously [21]. Arterial hemoglobin saturation (SpO_2) was measured with Masimo SET (Masimo Corp., Irvine, CA, USA) [22].

2.5. Statistics

Statistical analysis was performed on paired observations using Bonferoni's test after one-way ANOVA.

3. Results

3.1. BMT promotes survival and growth of laminin-α2-deficient mice

We first examined whether BMT affects lifespan in the *mdx* mice and *dy* mice. Kaplan–Meier survival curves revealed that a large percentage of control *dy* mice died around the first 20 weeks after birth (Fig. 1), whereas *dy* mice that received BMT survived up to 40 weeks, or almost double the lifespan of control *dy* mice. In *mdx* mice, we kept both groups of mice up to 2 years and found no difference for lifespan between BMT and control groups. These results indicate that BMT eliminated early death of *dy* mice.

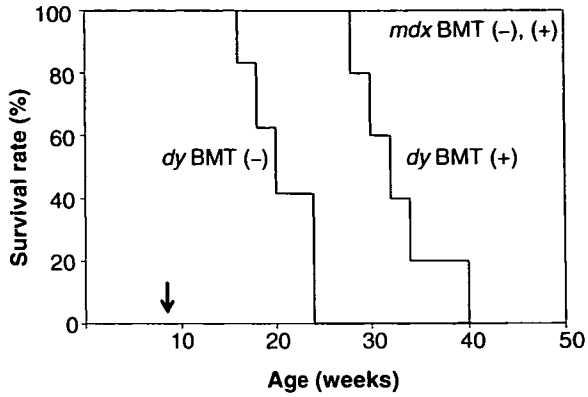

Fig. 1. Kaplan–Meier survival curves for BMT or non-treated control groups of each model of mice ($n = 10$, each). Arrow indicates 8 weeks of age at the time of BMT was performed. BMT (–), control group; BMT (+), treated group.

We further examined progressive changes in body weight of these models. BMT did not affect the growth rate of *mdx* mice in both males and females (Fig. 2A). The *dy* mice that received BMT lost weight right after BMT but gained weight more quickly and grew significantly larger than non-treated littermates (Fig. 2B). This tendency was found in both males and females. Thus, in addition to increasing lifespan, BMT improved the growth of *dy* mice.

3.2. BMT dose not significantly alter pathology in mdx muscle

We then questioned weather BMT improves muscle pathology of *mdx* mice. We examined diaphragm muscle, known to

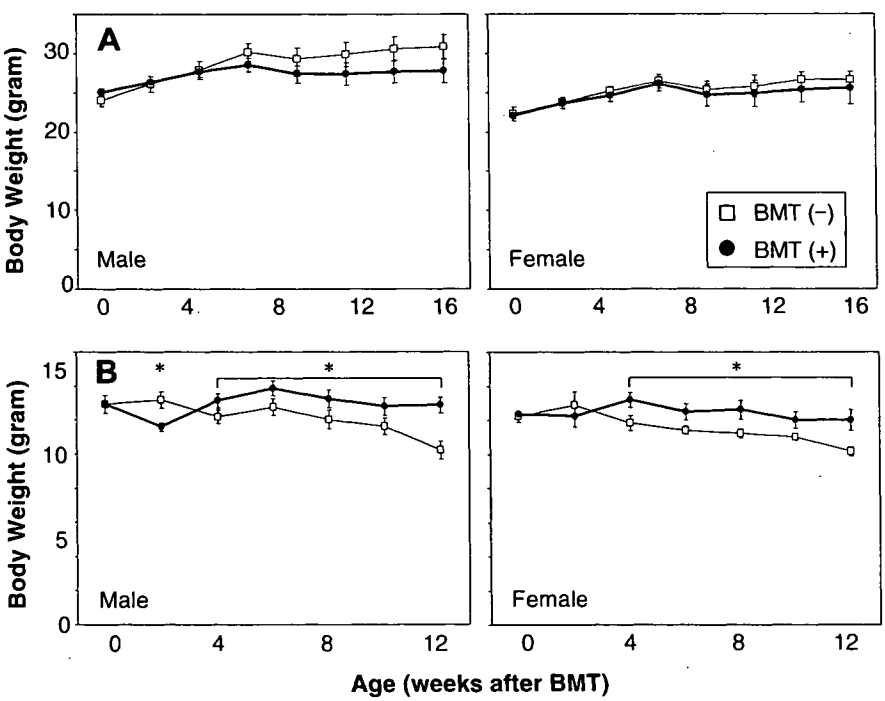

Fig. 2. (A) Growth curves for *mdx* mice between the control and BMT groups in males or females up to 16 weeks after BMT ($n = 5$, each). (B) Growth curves for *dy* mice until 12 weeks after BMT ($n = 5$, each). Data are expressed as means ± S.D. $^*P < 0.05$, Bonferoni's test after one-way ANOVA. BMT (–), control group; BMT (+), treated group.

the most severely damaged muscle in *mdx* mice [23]. H&E staining of diaphragm muscles both in BMT and control groups showed characteristic of dystrophic change including fiber size variability, central nucleus, fibrosis and fatty replacement. There is no detectable difference in gross pathology between both groups (data not shown). Next, diaphragm muscle sections of wild-type, control, and BMT group were stained for GFP and dystrophin immunoreactivity and DAPI (Fig. 3). We successfully obtained GFP-positive muscle fiber generation in irradiated BM chimeras. The frequency of GFP-positive fibers in diaphragm muscle was 4.9 ± 2.2% of total muscle fibers ($n = 3$). The frequency of dystrophin-positive fibers in diaphragm muscle was 0.9 ± 0.1% ($n = 3$). Merge images of *mdx* mice that underwent BMT revealed few GFP-positive fibers with dystrophin expression restored. Although some GFP-positive BM-derived skeletal muscles were observed, dystrophin expression was limited in *mdx* mice. These results indicate that muscle pathology was not significantly improved by BMT in *mdx* mice.

3.3. BMT improves pathology and significantly restores laminin-α2 expression in dy muscle

We next examined muscle pathology of *dy* mice. H&E staining of diaphragm muscles of *dy* mice in control group showed degenerative changes and atrophy in comparison with wild-type mice. Although degenerative changes are still observed, thickness of diaphragm muscles of *dy* mice is restored close to that of wild-type mice after BMT (Fig. 4A). We immunostained muscle sections of wild-type and *dy* mice (both control and BMT groups) with GFP and laminin-α2 antibodies and DAPI (Fig. 4B). The frequency of GFP-positive fibers in diaphragm muscle was 61.7 ± 5.9% of total muscle fibers ($n = 3$). The frequency of laminin-α2-positive fibers in diaphragm muscle was 82.6 ± 3.9% ($n = 3$). The merge image showed a significant number of GFP-positive fibers with laminin-α2 expression. Of particular importance, laminin-α2 expression was restored not only in GFP-positive fibers but also in GFP-negative fibers. In contrast to *mdx* mice, BM cells engrafted into skeletal muscle of *dy* mice with robust GFP-positive cells and laminin-α2 expression was significantly restored.

3.4. BMT improved muscle strength in dy mice

We measured the peak force of grip strength of mice. The grip strength of the *dy* mice that underwent BMT was significantly stronger ($P < 0.05$) than the *dy* control mice at 12 weeks after BMT (Fig. 5B). On the other hand, there were no substantial differences between the two groups of *mdx* mice (Fig. 5A). The ratio of grip strength per body weight revealed that BM transplanted *dy* mice had restored the ratio close to that of wild-type and *mdx* mice (Fig. 5C).

3.5. BMT improved respiratory function of dy mice

The SpO_2 measurements of *mdx* mice revealed no significant differences between control and BMT groups (Fig. 6A). In contrast, *dy* mice underwent BMT retained higher oxygen

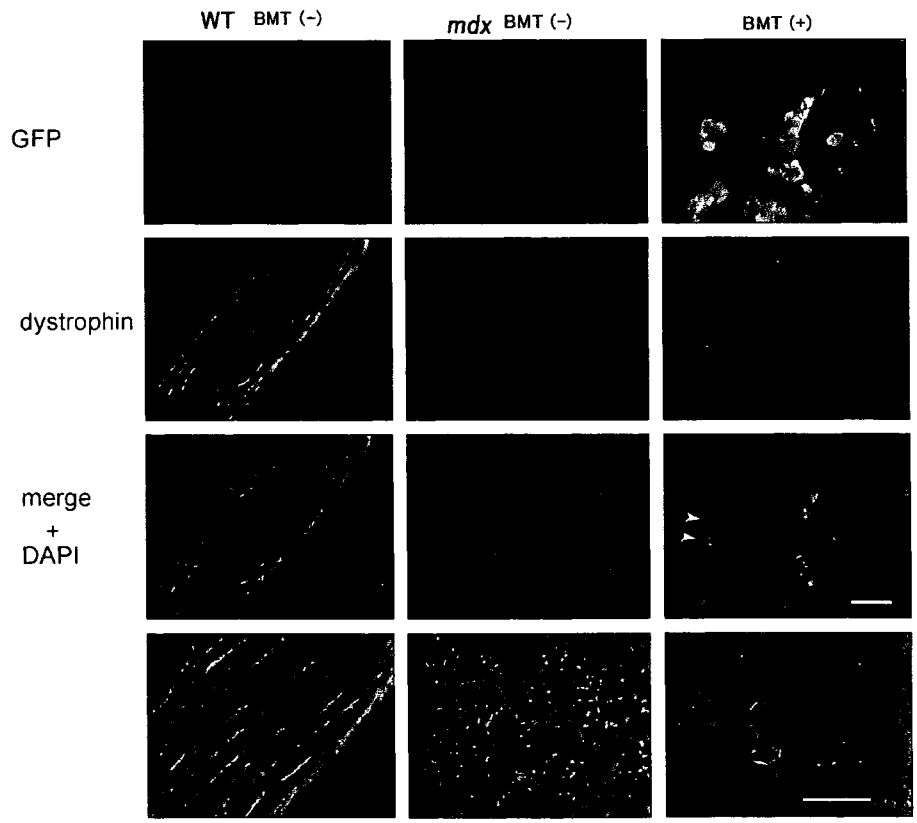

Fig. 3. Immunohistochemistry of diaphragm muscle sections of wild-type (WT-control, left column), control (*mdx*-control, middle column) or BMT group (*mdx*-BMT, right column). Merge image of *mdx*-BMT revealed that some GFP-positive fibers with dystrophin expression were restored (arrow heads). Bottom row is higher magnification of merge image. Bars: 100 μm. BMT (−), control group; BMT (+), treated group.

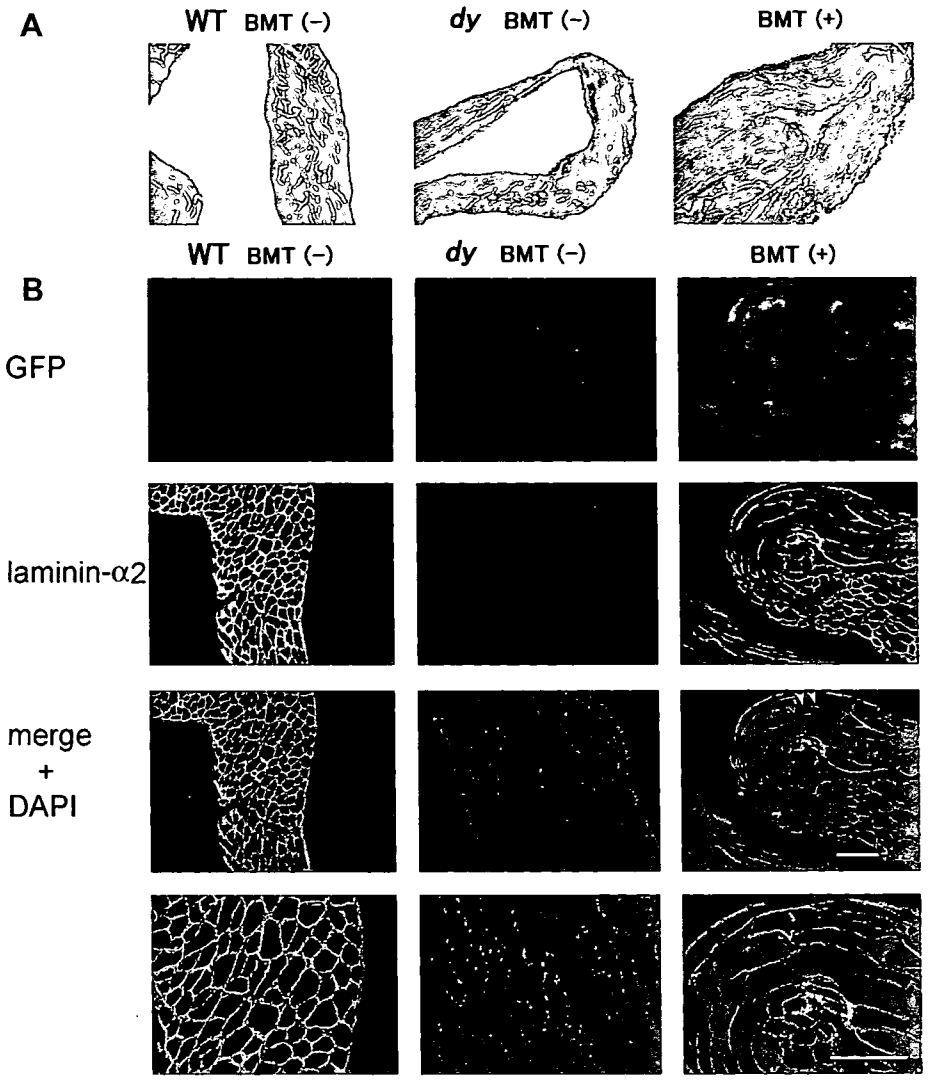

Fig. 4. BMT improved histopathology of *dy* muscles. (A) H&E staining of diaphragm muscle sections of wild-type (WT-control, left column), control (*dy*-control, middle column), or BMT group (*dy*-BMT, right column). (B) Immunohistochemistry of diaphragm muscle sections of wild-type (WT-control, left column), control (*dy*-control, middle column), or BMT group (*dy*-BMT, right column). Note that merge image of *dy*-BMT revealed a significant number of GFP-positive fibers with laminin-α2 expression. Of particular importance, laminin-α2 expression was restored not only in GFP-positive fibers but also in GFP-negative fibers (arrow heads). Bottom row is higher magnification of merge image. Bars: 100 μm. BMT (−), control group; BMT (+), treated group.

saturation and control *dy* mice showed decreased hypoxia at 20 weeks of age (12 weeks after BMT) (Fig. 6B).

4. Discussion

We found that BMT led to no significant improvements in muscle pathology of *mdx* mice. This result is consistent with recent reports [12–15]. We also found there was some discrepancy between GFP and dystrophin expressions in *mdx* mice that received BMT. This discrepancy is similar to that of a recent report describing that up to 5% of total muscle fibers expressed GFP, whereas dystrophin restoration after BMT was always <1% of total muscle fibers [24]. We also demonstrated that BMT failed to affect lifespan, growth rate, grip strength, and respiratory function of *mdx* mice. Taken together, BMT is unlikely to significantly ameliorate pathogenesis in dystrophin-deficient muscle.

In contrast to *mdx* mice, BMT led to a significant increase in lifespan and an increased growth rate of *dy* mice. Diaphragm muscle pathology of *dy* mice was also improved by BMT. Of particular significance is that laminin-α2, which is deficient in *dy* mice, was restored not only in GFP-positive myofibers but also GFP-negative myofibers. Additionally, BMT improved muscle strength and respiratory function of *dy* mice. This is the first report to demonstrate that BMT improves clinical symptoms of a mouse model of muscular dystrophy. Our study indicates that muscular dystrophy due to loss of laminin-α2 can be significantly ameliorated by BMT. Thus BMT could be an effective therapy for laminin-α2-deficient muscular dystrophy.

The reason why BMT was effective in *dy* mice but not *mdx* mice remains to be clarified. Two possible mechanisms to correct dystrophic pathology in *dy* mice by BMT are considered. First, the circulating BM-derived cells more easily fuse into host dystrophic cells through disrupted basal lamina in

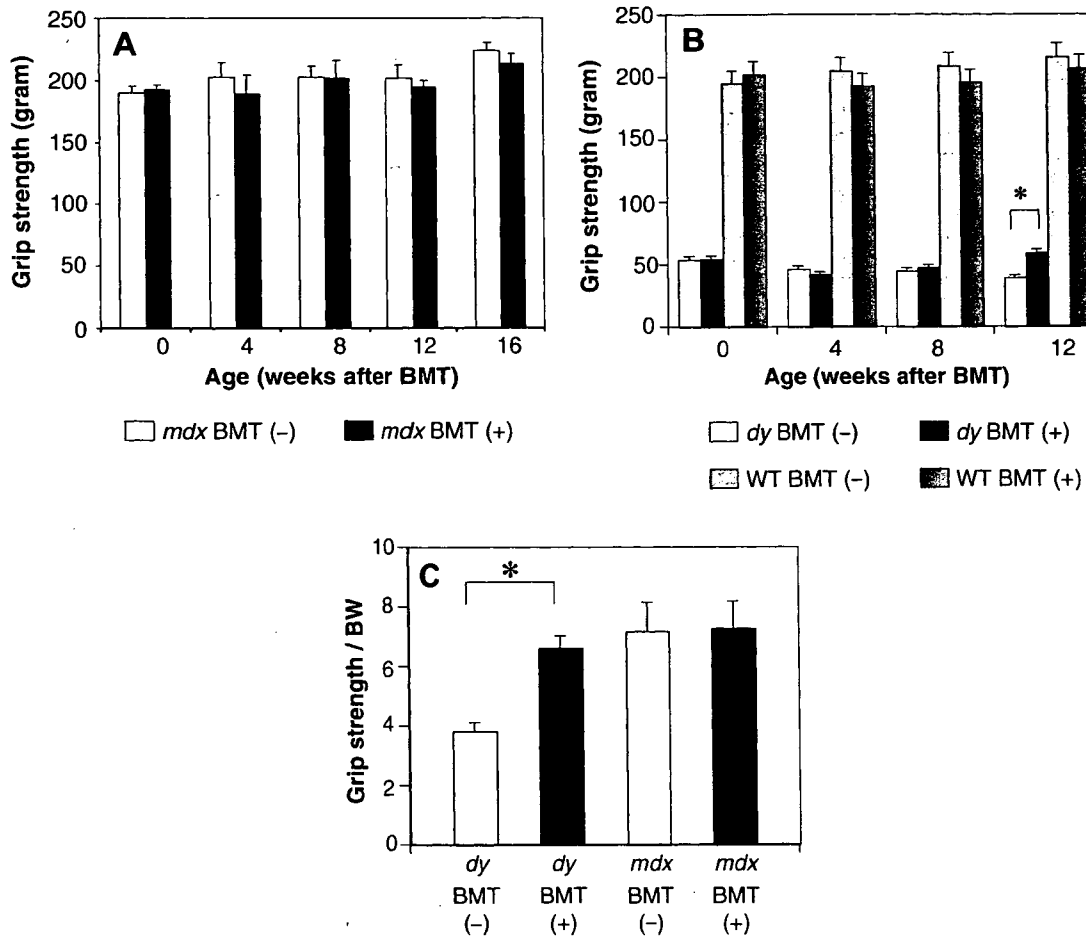

Fig. 5. Peak force measurement (g) of grip strength. (A) *mdx* mice before, 4, 8, 12, and 16 weeks after BMT ($n = 7$, each). (B) *dy* mice before, 4, 8, and 12 weeks after BMT ($n = 7$, each). Note that the grip strength of *dy*-BMT mice was significantly stronger than *dy*-control mice at 12 weeks after BMT. (C) Representation of grip strength per body weight of each group. Data are expressed as means ± S.D. $^*P < 0.05$, Bonferoni's test after one-way ANOVA. BMT (−), control group; BMT (+), treated group.

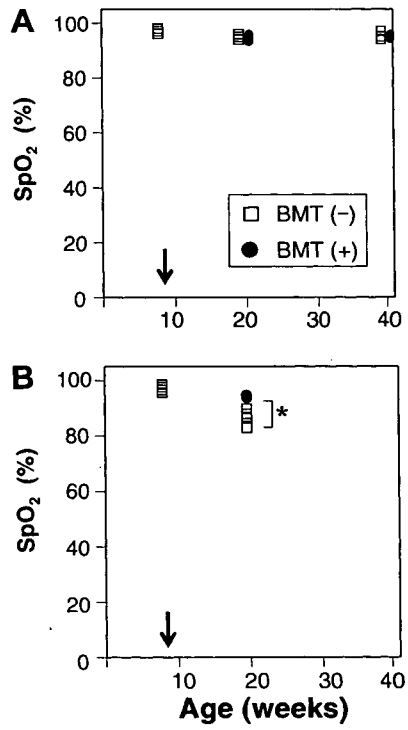

dy skeletal muscles. Second, laminin-α2 molecules produced by BM-derived cells diffuse in the vicinity to form normal laminin-2 networks even in GFP-negative myofibers. In contrast, in *mdx* mice, the basal lamina is so well-preserved that foreign BM-derived cells could not integrate into recipient cells.

In addition to MDC1A, BMT could be effective for other types of dystrophy including Fukuyama congenital muscular dystrophy, muscle-eye-brain disease, and Walker–Warburg syndrome in which partial laminin-α2 deficiency and disruption of basal lamina are commonly observed [25].

In conclusion, on the basis of our results, BMT may be more successful in the treatment of muscle diseases such as MDC1A than DMD.

Fig. 6. SpO_2 measurements. (A) *mdx* mice before and 12 and 32 weeks after BMT ($n = 5$, each). (B) *dy* mice before BMT and 12 weeks after BMT. Note that SpO_2 of *dy*-BMT group retained higher oxygen saturation whereas the *dy*-control group showed a decrease in hypoxia ($n = 5$, each). Arrow indicates 8 weeks of age at the time of BMT was performed. BMT (−), control group; BMT (+), treated group.

Acknowledgments: We thank Drs. Shin-ichiro Nishimatsu and Daigo Hashimoto for fruitful discussion. We thank Shizuka Sasano, Yayoi Mori, Nami Naoe, Yumi Naganuma, Megumu Kita for their technical assistance. This work was supported by a Research Grant (17A-10) for Nervous and Mental Disorders from the Ministry of Health, Labour and Welfare; Grants (15131301 and 17231401) for Research on Psychiatric and Neurological Diseases and Mental Health from the Ministry of Health, Labour and Welfare of Japan and from JSPS KAKENHI (16590856); and by Research Project Grants (16-601 and 17-610S) from Kawasaki Medical School.

References

[1] Emery, A.E. (2002) The muscular dystrophies. Lancet 359, 687–695.
[2] Engel, A.G. and Ozawa, A. (2004) Dystrophinopathies in: Myology (Engel, A.G. and Franzini-Armstrong, C., Eds.), pp. 961–1025, McGraw Hill, New York.
[3] Kirschner, J. and Bonnemann, C.G. (2004) The congenital and limb-girdle muscular dystrophies: sharpening the focus, blurring the boundaries. Arch. Neurol. 61, 189–199.
[4] Nonaka, I. (1998) Animal models of muscular dystrophies. Lab. Anim. Sci. 48, 8–17.
[5] Ryder-Cook, A.S., Sicinski, P., Thomas, K., Davies, K.E., Worton, R.G., Barnard, E.A., Darlison, M.G. and Barnard, P.J. (1988) Localization of the mdx mutation within the mouse dystrophin gene. EMBO J. 7, 3017–3021.
[6] Xu, H., Wu, X.R., Wewer, U.M. and Engvall, E. (1994) Murine muscular dystrophy caused by a mutation in the laminin alpha 2 (Lama2) gene. Nat. Genet. 8, 297–302.
[7] Sunada, Y., Bernier, S.M., Kozak, C.A., Yamada, Y. and Campbell, K.P. (1994) Deficiency of merosin in dystrophic dy mice and genetic linkage of laminin M chain gene to dy locus. J. Biol. Chem. 269, 13729–13732.
[8] Chakkalakal, J.V., Thompson, J., Parks, R.J. and Jasmin, B.J. (2005) Molecular, cellular, and pharmacological therapies for Duchenne/Becker muscular dystrophies. FASEB J. 19, 880–891.
[9] Prockop, D.J. (1997) Marrow stromal cells as stem cells for nonhematopoietic tissues. Science 276, 71–74.
[10] Pittenger, M.F. et al. (1999) Multilineage potential of adult human mesenchymal stem cells. Science 284, 143–147.
[11] Ferrari, G. and Mavilio, F. (2002) Myogenic stem cells from the bone marrow: a therapeutic alternative for muscular dystrophy? Neuromuscul. Disord. 12 (Suppl 1), S7–S10.
[12] Ferrari, G., Cusella-De Angelis, G., Coletta, M., Paolucci, E., Stornaiuolo, A., Cossu, G. and Mavilio, F. (1998) Muscle regeneration by bone marrow-derived myogenic progenitors. Science 279, 1528–1530.
[13] Bittner, R.E. et al. (1999) Recruitment of bone-marrow-derived cells by skeletal and cardiac muscle in adult dystrophic mdx mice. Anat. Embryol. (Berl.) 199, 391–396.
[14] Gussoni, E., Soneoka, Y., Strickland, C.D., Buzney, E.A., Khan, M.K., Flint, A.F., Kunkel, L.M. and Mulligan, R.C. (1999) Dystrophin expression in the mdx mouse restored by stem cell transplantation. Nature 401, 390–394.
[15] Fukada, S. et al. (2002) Muscle regeneration by reconstitution with bone marrow or fetal liver cells from green fluorescent protein-gene transgenic mice. J. Cell Sci. 115, 1285–1293.
[16] Gussoni, E. et al. (2002) Long-term persistence of donor nuclei in a Duchenne muscular dystrophy patient receiving bone marrow transplantation. J. Clin. Invest. 110, 807–814.
[17] Okabe, M., Ikawa, M., Kominami, K., Nakanishi, T. and Nishimune, Y. (1997) 'Green mice' as a source of ubiquitous green cells. FEBS Lett. 407, 313–319.
[18] Blazar, B.R., Roopenian, D.C., Taylor, P.A., Christianson, G.J., Panoskaltsis-Mortari, A. and Vallera, D.A. (1996) Lack of GVHD across classical, single minor histocompatibility (miH) locus barriers in mice. Transplantation 61, 619–624.
[19] Teshima, T., Ordemann, R., Reddy, P., Gagin, S., Liu, C., Cooke, K.R. and Ferrara, J.L. (2002) Acute graft-versus-host disease does not require alloantigen expression on host epithelium. Nat. Med. 8, 575–581.
[20] Sunada, Y. et al. (2001) Transgenic mice expressing mutant caveolin-3 show severe myopathy associated with increased nNOS activity. Hum. Mol. Genet. 10, 173–178.
[21] Tagawa, K. et al. (2000) Myopathy phenotype of transgenic mice expressing active site-mutated inactive p94 skeletal muscle-specific calpain, the gene product responsible for limb girdle muscular dystrophy type 2A. Hum. Mol. Genet. 9, 1393–1402.
[22] Hummler, H.D., Engelmann, A., Pohlandt, F., Hogel, J. and Franz, A.R. (2004) Accuracy of pulse oximetry readings in an animal model of low perfusion caused by emerging pneumonia and sepsis. Intensive Care Med. 30, 709–713.
[23] Stedman, H.H. et al. (1991) The mdx mouse diaphragm reproduces the degenerative changes of Duchenne muscular dystrophy. Nature 352, 536–539.
[24] Chretien, F., Dreyfus, P.A., Christov, C., Caramelle, P., Lagrange, J.L., Chazaud, B. and Gherardi, R.K. (2005) In vivo fusion of circulating fluorescent cells with dystrophin-deficient myofibers results in extensive sarcoplasmic fluorescence expression but limited dystrophin sarcolemmal expression. Am. J. Pathol. 166, 1741–1748.
[25] Hayashi, Y.K., Engvall, E., Arikawa-Hirasawa, E., Goto, K., Koga, R., Nonaka, I., Sugita, H. and Arahata, K. (1993) Abnormal localization of laminin subunits in muscular dystrophies. J. Neurol. Sci. 119, 53–64.

Muscular atrophy of caveolin-3–deficient mice is rescued by myostatin inhibition

Yutaka Ohsawa,[1] Hiroki Hagiwara,[1] Masashi Nakatani,[2] Akihiro Yasue,[3] Keiji Moriyama,[3] Tatsufumi Murakami,[1] Kunihiro Tsuchida,[2] Sumihare Noji,[4] and Yoshihide Sunada[1]

[1]Division of Neurology, Department of Internal Medicine, Kawasaki Medical School, Kurashiki, Japan. [2]Division for Therapies against Intractable Diseases, Institute for Comprehensive Medical Science, Fujita Health University, Toyoake, Japan. [3]Department of Orthodontics, Faculty of Dentistry, and [4]Department of Biological Science and Technology, Faculty of Engineering, The University of Tokushima, Tokushima, Japan.

Caveolin-3, the muscle-specific isoform of caveolins, plays important roles in signal transduction. Dominant-negative mutations of the *caveolin-3* gene cause autosomal dominant limb-girdle muscular dystrophy 1C (LGMD1C) with loss of caveolin-3. However, identification of the precise molecular mechanism leading to muscular atrophy in caveolin-3–deficient muscle has remained elusive. Myostatin, a member of the muscle-specific TGF-β superfamily, negatively regulates skeletal muscle volume. Here we report that caveolin-3 inhibited myostatin signaling by suppressing activation of its type I receptor; this was followed by hypophosphorylation of an intracellular effector, Mad homolog 2 (Smad2), and decreased downstream transcriptional activity. Loss of caveolin-3 in P104L mutant caveolin-3 transgenic mice caused muscular atrophy with increase in phosphorylated Smad2 (p-Smad2) as well as *p21* (also known as *Cdkn1a*), a myostatin target gene. Introduction of the myostatin prodomain, an inhibitor of myostatin, by genetic crossing or intraperitoneal administration of the soluble type II myostatin receptor, another inhibitor, ameliorated muscular atrophy of the mutant caveolin-3 transgenic mice with suppression of p-Smad2 and *p21* levels. These findings suggest that caveolin-3 normally suppresses the myostatin-mediated signal, thereby preventing muscular atrophy, and that hyperactivation of myostatin signaling participates in the pathogenesis of muscular atrophy in a mouse model of LGMD1C. Myostatin inhibition may be a promising therapy for LGMD1C patients.

Introduction

Caveolins are 21- to 24-kDa integral membrane proteins and are principal components of flask-shaped invaginations of the plasma membrane known as caveolae. These proteins play important roles in signal transduction and vesicular trafficking (1–3). They directly bind to and regulate specific lipid and lipid-modified molecules including cholesterol, G proteins, G protein–coupled receptors, Src family protein kinases, Ha-Ras, and nitric oxide synthases (1, 2). The interaction between caveolin and lipid-modified proteins is mediated by a specific caveolin-binding motif on the target protein and by a scaffolding domain in caveolin (3). There are 3 mammalian caveolin genes, namely, *caveolin-1*, *-2*, and *-3*. Caveolin-1 and -2 are coexpressed and form heterooligomers in nonmuscle cells whereas caveolin-3 is muscle specific and forms homooligomers in muscle cells (1, 2).

Loss of caveolin-3 resulting from dominant-negative mutations of the *caveolin-3* gene causes autosomal dominant limb-girdle muscular dystrophy 1C (LGMD1C) (4). We previously generated Tg mice overexpressing the Pro104Leu mutant caveolin-3 (CAV-3^{P104L}) as a model for LGMD1C (5). The skeletal muscle pathology of the Tg mice includes myopathy characterized by severe skeletal muscle atrophy and a deficiency in caveolin-3. We also found a significant increase in neuronal nitric oxide synthase activity in their skeletal muscle. Other groups have demonstrated mislocalization of Src and dysferlin to the Golgi apparatus (6, 7). Despite these findings, the precise molecular mechanism leading to muscular atrophy in caveolin-3–deficient skeletal muscle remains to be elucidated.

Myostatin is a member of the TGF-β superfamily and plays an essential role in the negative regulation of skeletal muscle volume (8). Overexpression of myostatin causes severe muscular atrophy (9, 10) whereas targeted disruption of myostatin markedly increases muscle mass in mice (8, 11). We also generated Tg mice overexpressing the myostatin prodomain in skeletal muscle ($Mstn^{Pro}$) (12), an inhibitor of myostatin activation (13–17). Like other TGF-β superfamily members (18), myostatin is synthesized as a precursor protein and undergoes proteolytic processing to generate an N terminal prodomain and a biologically active, C terminal disulfide-linked dimer (19). In the inactive state, the prodomain binds to the C terminal myostatin dimer and strongly inhibits its biological activity (13). The circulating active form of myostatin directly binds to and activates activin receptor IIB (ActRIIB), a type II serine/threonine kinase receptor (19). This, in turn, activates the type I serine/threonine kinase receptor activin receptor–like kinase 4 (ALK4) or ALK5 at the plasma membrane (20, 21). The activation of a heteromeric receptor complex consisting of type II and type I serine/threonine kinase receptors induces the phosphorylation of intracellular effectors Mad homolog 2 (Smad2) and Smad3 (20, 21). Phosphorylated Smad2 and Smad3 translocate from the cytoplasm to the nucleus, where they regulate the transcription of specific target genes (20–22).

Recently, caveolin-1 was reported to inhibit the activation of the type I receptor for TGF-β1, which induces growth arrest in nonmuscle cells (23). Upon consideration of molecular analogy and tissue distribution, we hypothesized that caveolin-3 inhibits myostatin signaling in muscle cells in a similar manner. Accordingly, an increase in myostatin activity resulting from loss of

Nonstandard abbreviations used: ActRIIB, activin receptor IIB; ALK4, activin receptor–like kinase 4; $Cav3^{P104L}$ mice, Tg mice overexpressing the P104L mutant caveolin-3; CDK, cyclin-dependent kinase; LGMD1C, limb-girdle muscular dystrophy 1C; $Mstn^{Pro}$ mice, Tg mice overexpressing the myostatin prodomain in skeletal muscle; p-, phosphorylated; Smad2, Mad homolog 2; TA, tibialis anterior.

Conflict of interest: The authors have declared that no conflict of interest exists.

Citation for this article: *J. Clin. Invest.* 116:2924–2934 (2006). doi:10.1172/JCI28520.